

An investigation of the hidden structure of states in a mean-field spin-glass model

This article has been downloaded from IOPscience. Please scroll down to see the full text article.

1997 J. Phys. A: Math. Gen. 30 7021

(<http://iopscience.iop.org/0305-4470/30/20/009>)

View [the table of contents for this issue](#), or go to the [journal homepage](#) for more

Download details:

IP Address: 171.66.16.110

The article was downloaded on 02/06/2010 at 06:03

Please note that [terms and conditions apply](#).

An investigation of the hidden structure of states in a mean-field spin-glass model

Andrea Cavagna[†], Irene Giardina[‡] and Giorgio Parisi[§]

Dipartimento di Fisica, Università di Roma I 'La Sapienza', P.le A. Moro 5, 00185 Roma, Italy
and INFN Sezione di Roma I, Roma, Italy

Received 9 June 1997

Abstract. We study the geometrical structure of the states in the low-temperature phase of a mean-field model for generalized spin glasses, the p -spin spherical model. This structure cannot be revealed by the standard methods, mainly due to the presence of an exponentially high number of states, each one having a vanishing weight in the thermodynamic limit. Performing a purely entropic computation, based on the TAP equations for this model, we define a constrained complexity which gives the overlap distribution of the states. We find that this distribution is continuous, non-random and highly dependent on the energy range of the considered states. Furthermore, we show which is the geometrical shape of the threshold landscape, giving some insight into the role played by threshold states in the dynamical behaviour of the system.

1. Introduction

Despite some recent developments [9, 10, 15], a deep understanding of the structure of the states in the p -spin spherical model is still lacking. The problem is the following.

In the context of the TAP approach [2], it has been shown that, in the temperature range between the static and the dynamical transition, this model has an exponentially high number of states (TAP solutions), with free-energy densities in a finite range $[f_{\min}, f_{\text{th}}]$. What happens is that *equilibrium* states at temperature T are not the lowest ones corresponding to f_{\min} , but rather those which optimize the balance between the free energy and the entropic contribution due to the presence of a great number of states with the same free energy. Thus equilibrium states are those which minimize the generalized free-energy density $\phi(f) = f - T\Sigma(f)$, where Σ is the *complexity*. The states with free-energy density f either lower or higher than the value which minimizes ϕ must be considered as metastable. On the other hand, *all* these states, the equilibrium as well as the metastable ones, singularly taken have a vanishing weight in the thermodynamic limit. In this sense, an equilibrium state is not different from a metastable state, since the equilibrium condition is a fully collective effect [9, 18].

It is clear that the presence of this huge number of states makes it interesting to know how they are disposed in the phase space, and therefore to investigate their distribution and structure.

To clarify what we intend with the structure of the states it is useful to consider the Sherrington–Kirkpatrick (SK) model [1]. In this case, in the context of the replica method,

[†] E-mail address: andrea.cavagna@roma1.infn.it

[‡] E-mail address: irene.giardina@roma1.infn.it

[§] E-mail address: giorgio.parisi@roma1.infn.it

the solution given in [3–5] made it possible to define and calculate the overlap distribution $P(q)$ of the pure states: $P(q)$ is defined as the probability that, drawn two states, their mutual overlap is equal to q . Therefore, in the distribution $P(q)$ two different contributions are present: the existence of states having mutual overlap q and their individual statistical weights. The function $P(q)$ gives for the SK model important structural information on the distribution of the states in terms of the overlap [23].

For the p -spin spherical model we would like to have structural information of the same kind as that given by the distribution $P(q)$ for the SK model.

Unfortunately, it is known that by applying the standard replica method to the p -spin spherical model a trivial result is obtained [8]: in the intermediate-temperature phase that we are considering, the model is solved by a replica-symmetric solution, corresponding to a trivial distribution function $P(q) = \delta(q)$. This delta function simply means that the *typical* overlap between two states is zero. On the other hand, let us consider why this distribution does not get any contribution from the self overlap of the equilibrium states, which is different from zero. The answer is that all these states singularly have a weight so low that the contribution of their self overlap is not present in the distribution $P(q)$. In other words, it is highly unlikely to draw the same state twice and measure its self overlap, if this is either an equilibrium state or a metastable one.

For the same reason it is possible that the distribution $P(q)$ does not catch a contribution from *all* the other possible values of the overlap q , simply because obtaining two states with an overlap different from zero has a vanishing probability in the thermodynamic limit. This would mean that the trivial form of $P(q)$ is not a consequence of the absence of states with mutual overlap different from zero, but rather of the difficulty of finding them [13]. On the contrary, there is the possibility that indeed *all* the states of this model have a mutual overlap of zero, i.e. that states with an overlap different from zero do not exist at all. In this last case it is clear that there would be only a trivial structure of the states, exactly reproduced by a trivial $P(q)$. The standard static approaches cannot distinguish between these two pictures, and more than this, in the case in which a non-trivial hidden structure were present, they are not able to give us any insight into the problem. In our opinion it seemed very strange to have this huge number of states without any interesting geometrical structure and therefore we have tried to develop some non-standard methods which could provide some information on this topic.

The first question to answer is then: Does a non-trivial structure of the states exist? This question has been partially answered in the context of the real replica method, by the definition of a three-replica potential [15]. Within this method it has been possible to demonstrate that, given an equilibrium state, there are both metastable and equilibrium states with *any* value of the overlap q , up to a certain maximum value. This shows clearly that a non-trivial structure of the states for this model is present, and that the second picture we have stated above has to be discarded. On the other hand, the shape of the energy spectrum of the states found with this method was not completely understood, moreover there was no control on the choosing procedure of the detected states.

Therefore, it is necessary to define a tool by which the hidden structure of the states for the p -spin spherical model can be analysed in a deep way. Yet, as we have seen, there is the problem of the vanishing weight of these states that leads to the trivial form of the standard distribution function $P(q)$.

Bearing this in mind, the most natural thing to do is to perform a purely entropic computation, disregarding the thermodynamic weight of the states. Thus, what we have done is to fix a reference state in the phase space and simply *count* how many states of a given kind are present at overlap q with that state. More precisely, what we have actually

computed is the number of TAP solutions having a given overlap q with a single fixed solution. The resulting quantity is what we have called the *constrained complexity* Σ_c .

To conclude this introduction we want to stress a point that could seem trivial, but that has some importance in our opinion. We said that we wanted to study the structure of the *states* of this model, but actually we work with *solutions* of the TAP equations. The underlying hypothesis is then that TAP solutions really correspond to thermodynamic states, intended as local minima of the *true* free energy of the system. This is not a trivial identification, but it has been confirmed in various ways [10, 11, 15]. For example, in the case of the three-replica potential of [15], one can show that the local minima of the potential, which correspond to metastable states of the system, always have a free energy and a self overlap that satisfy TAP equations.

The paper is organized in the following way. In section 2 we define the constrained complexity and describe the way in which the calculation has been performed. The main results are exposed in section 3, where the behaviour of Σ_c is analysed and interpreted in terms of geometrical structure of the states. In section 4 we address the question of which are the dominant states at a certain distance from a reference equilibrium state, while in section 5 we focus on the structure of the threshold states, which are important in many respects. In section 6 we state the conclusions and outline the most important open problems. Finally, the comparison with the results of the real replica method is carried out in a detailed way in the appendix.

2. The constrained complexity

The p -spin spherical model is defined by the following Hamiltonian

$$H(s) = - \sum_{i_1 < \dots < i_p} J_{i_1 \dots i_p} s_{i_1} \dots s_{i_p} \quad (2.1)$$

where the spins s are real variables satisfying the spherical constraint $\sum_i s_i^2 = N$ (N is the size of the system) and the couplings J are Gaussian variables with zero mean and variance $p!/2N^{p-1}$ [7, 8, 14].

In the frame of the TAP approach [2], one formulates mean-field equations for the local magnetizations $m_i = \langle s_i \rangle$ of the system. In [9] a free-energy density, f_{TAP} , has been introduced as a function of the magnetizations m_i : the minimization of f_{TAP} with respect to m_i gives the TAP equations of the system. Solving these equations at $T = 0$ one finds minima of f_{TAP} with the energy density included in a finite range $[E_{\text{min}}, E_{\text{th}}]$. The solutions with the highest energy density E_{th} are usually called *threshold* solutions. For each value of the energy density E in this range, there is an exponentially high number of solutions

$$\mathcal{N}(E) \sim e^{N\Sigma(E)} \quad (2.2)$$

where $\Sigma(E)$ is the *complexity* of the class of TAP solutions corresponding to that particular energy. The complexity $\Sigma(E)$ for this model has been computed in [12], where it is found that Σ is an increasing function of E , which is zero for $E = E_{\text{min}}$ and reaches a finite value for $E = E_{\text{th}}$. Moreover, due to the particular homogeneity of the Hamiltonian, there is a one-to-one mapping of the solutions found at temperature zero, into solutions at finite temperature T , with neither splitting nor merging of solutions with varying the temperature. Due to this, TAP equations at $T = 0$ can be solved, obtaining a class of solutions with a certain zero-temperature energy density E and then transport these solutions to finite T . Therefore, from now on we will identify a TAP solution with its zero-temperature energy density E , even if we are considering this solution at finite temperature T . The important

thing is that the complexity $\Sigma(E)$ of a given class does not depend on T , but only on the zero-temperature energy E of this class, while the self overlap of each solution depends both on E and on the temperature T .

We now introduce the constrained complexity:

$$\Sigma_c(E_2, q|E_1) \stackrel{\text{def}}{=} \lim_{N \rightarrow \infty} \frac{1}{N} \overline{\log \mathcal{N}(E_2, q|E_1)}. \quad (2.3)$$

In this definition $\mathcal{N}(E_2|q, E_1)$ is the number of TAP solutions with energy density E_2 having overlap q with a single fixed solution of energy density E_1 . The bar indicates the average over the disorder. What we are doing here is to fix a single state of energy E_1 and simply count how many states of energy E_2 are found at overlap (distance) q with it. We remark that q is the overlap between these TAP solutions at finite temperature, while E_1 and E_2 are their zero-temperature energy densities.

In definition (2.3) we have averaged the logarithm of \mathcal{N} , since we expect that this is the extensive quantity. Therefore, to perform this average it is necessary to introduce replicas. However, it can be shown that, in the unconstrained case [12], the correct ansatz for the overlap matrix is symmetric and diagonal and this is equivalent to directly averaging the number \mathcal{N} of the solutions. In our case the same prescription leads to the following definition:

$$\Sigma_c(E_2, q|E_1) \stackrel{\text{def}}{=} \lim_{N \rightarrow \infty} \frac{1}{N} \log \overline{\mathcal{N}(E_2, q|E_1)} \quad (2.4)$$

and this is the quantity we shall compute. It is surely possible that the introduction of the constraint q requires a breaking of the replica symmetry and therefore definition (2.4) has to be considered as a first approximation. Yet, as we shall show, the results obtained with formula (2.4) suggest that this is a good approximation.

The complexity Σ_c can be obtained by counting all pairs of solutions with energies (E_1, E_2) at mutual overlap q and dividing it by the number of solutions with energy E_1 , i.e.

$$\Sigma_c(E_2, q|E_1) = \lim_{N \rightarrow \infty} \left\{ \frac{1}{N} \log \overline{\mathcal{N}(E_1, E_2, q)} - \frac{1}{N} \log \overline{\mathcal{N}(E_1)} \right\} \stackrel{\text{def}}{=} \Gamma(E_1, E_2, q) - \Sigma(E_1) \quad (2.5)$$

where $\Sigma(E_1)$ is the usual unconstrained complexity computed in [12]. We note that the quantity Γ is symmetric in (E_1, E_2) while Σ_c is not. Moreover, $\Gamma(E_1, E_2, 0) = \Sigma(E_1) + \Sigma(E_2)$, since *almost* all TAP solutions are mutually orthogonal, and then

$$\Sigma_c(E_2, 0|E_1) = \Sigma(E_2). \quad (2.6)$$

This is the first check we have to face in our calculation.

Let $m_i^{(1)}$ and $m_i^{(2)}$ be two solutions with self overlaps q_1 and q_2 , and mutual overlap q ; using the notation $m \cdot m' = \sum_i m_i m'_i$, we have

$$m^{(1)} \cdot m^{(1)} = Nq_1 \quad m^{(2)} \cdot m^{(2)} = Nq_2 \quad m^{(1)} \cdot m^{(2)} = Nq. \quad (2.7)$$

Following [9] we write TAP equations in terms of the angular part of the magnetizations m_i

$$\sigma_i = \frac{m_i^{(1)}}{\sqrt{q_1}} \quad \tau_i = \frac{m_i^{(2)}}{\sqrt{q_2}} \quad (2.8)$$

for which it holds

$$\sigma \cdot \sigma = N \quad \tau \cdot \tau = N \quad \sigma \cdot \tau = N \frac{q}{\sqrt{q_1 q_2}} \stackrel{\text{def}}{=} Nq_0. \quad (2.9)$$

In terms of the angular variables σ and τ , the TAP equations read

$$0 = -p \sum_{i_2 < \dots < i_p} J_{i_1 i_2 \dots i_p} \sigma_{i_2} \dots \sigma_{i_p} - p E_1 \sigma_{i_1} \stackrel{\text{def}}{=} \mathcal{T}_i(\sigma; E_1) \quad i = 1, \dots, N \quad (2.10)$$

where E_1 is the zero-temperature energy density

$$E_1 = -\frac{1}{N} \sum_{i_1 < \dots < i_p} J_{i_1 \dots i_p} \sigma_{i_1} \dots \sigma_{i_p}. \quad (2.11)$$

Relations of the same kind of (2.10) and (2.11) hold for τ and E_2 . It is now possible to write Γ with the standard method of [12, 16] in the following way:

$$\begin{aligned} \Gamma(E_1, E_2, q) &= \frac{1}{N} \log \int \mathcal{D}P(J) \int \mathcal{D}\sigma \mathcal{D}\tau \prod_i \delta(\mathcal{T}_i(\sigma; E_1)) \delta(\mathcal{T}_i(\tau; E_2)) \\ &\times \left| \det \left(\frac{\partial \mathcal{T}(\sigma; E_1)}{\partial \sigma} \right) \right| \left| \det \left(\frac{\partial \mathcal{T}(\tau; E_2)}{\partial \tau} \right) \right| \\ &\times \delta(\sigma \cdot \sigma - N) \delta(\tau \cdot \tau - N) \delta(\sigma \cdot \tau - N q_0) \end{aligned} \quad (2.12)$$

with

$$\mathcal{D}P(J) = \prod_{i_1 < \dots < i_p} \sqrt{\frac{N^{p-1}}{\pi p!}} \exp(-J_{i_1 \dots i_p}^2 N^{p-1}/p!) dJ_{i_1 \dots i_p}. \quad (2.13)$$

We note that the dependence on the temperature is entirely contained in q_0 through q_1 and q_2 , functions respectively of E_1 , E_2 and β [9].

In formula (2.12) we can drop the two moduli since it is possible to check *a posteriori* that the determinants are positive. Actually, this is a tricky point. As shown in [18, 19], if one counts the stationary points of a function neglecting the modulus in integrals of the kind (2.12), a trivial result is obtained, due to the Morse theorem. Nevertheless, we note that we are not calculating here the whole number of stationary points of the TAP free energy, but we are counting those *with a given energy density*. Moreover, for energies lower than the threshold, the dominant contribution to the determinant is truly positive, as can be shown by computing the Hessian spectrum of the TAP free energy. On the other hand, the same procedure of removing the modulus gives the normal unconstrained TAP complexity of [12], which has been confirmed in [10] with a totally different method.

In order to perform the calculation it is useful to write both these determinants by means of a fermionic representation

$$\det A = \int d\bar{\psi} d\psi e^{-\sum_{ij} \bar{\psi}_i A_{ij} \psi_j} \quad (2.14)$$

while the usual (bosonic) integral representation is adopted for the delta functions which implement the TAP equations in (2.12). The average over the disorder J generates couplings among bosonic and fermionic variables, but these mixed couplings are set equal to zero as in the unconstrained calculation. In this way it is possible to average separately the fermionic part from the bosonic part. This greatly simplifies the calculation, since it turns out that the fermionic part has exactly the same form as in the unconstrained case, while, due to the presence of the constraint q_0 , this is no longer true for the bosonic part. We can write the unconstrained complexity in the usual following way (see [12]):

$$\Sigma(E) = \Xi(E)_{\text{bosons}} + \Omega(E)_{\text{fermions}} \quad (2.15)$$

with

$$\Xi(E) = \frac{1}{2} \log(2/p) - \frac{1}{2} - E^2 \quad \Omega(E) = -pEz - \frac{p(p-1)}{4} z^2 - \log z \quad (2.16)$$

$$z = \frac{-E - \sqrt{E^2 - 2(p-1)/p}}{(p-1)}. \quad (2.17)$$

Similarly, for the above, we can write

$$\Gamma(E_1, E_2, q) = \Delta(E_1, E_2, q) + \Omega(E_1) + \Omega(E_2) \quad (2.18)$$

where Δ is the bosonic contribution to (2.12). In this way Σ_c has the form

$$\Sigma_c(E_2, q|E_1) = \Delta(E_1, E_2, q) - \Xi(E_1) + \Omega(E_2). \quad (2.19)$$

Besides the variables σ and τ there are two more bosonic fields coming from the integral representation of the delta functions, respectively μ and λ . All these bosons couple because of the average over the disorder J . To perform the saddle-point approximation we introduce the following set of variational parameters:

$$\begin{aligned} Nx_1 &= \mu \cdot \mu & Nx_2 &= \lambda \cdot \lambda & Nx_3 &= \mu \cdot \lambda \\ Ny_1 &= \sigma \cdot \mu & Ny_2 &= \tau \cdot \lambda & Ny_3 &= \sigma \cdot \lambda & Ny_4 &= \tau \cdot \mu. \end{aligned} \quad (2.20)$$

We recall that $\sigma \cdot \tau = Nq_0$, while $\sigma \cdot \sigma = \tau \cdot \tau = N$. The explicit calculation gives

$$\Delta(E_1, E_2, q) = \text{Exp}_{x,y} \left\{ ipE_1y_1 + ipE_2y_2 - \frac{p(p-1)}{2} q_0^{p-2} y_3y_4 - \frac{p}{4} (x_1 + x_2) \right. \quad (2.21)$$

$$\left. - \frac{p}{2} q_0^{p-1} x_3 - \frac{p(p-1)}{4} (y_1^2 + y_2^2) + \frac{1}{2} \log \left(\frac{\Lambda}{1 - q_0^2} \right) \right\} \quad (2.22)$$

with

$$\Lambda = [x_1(1 - q_0^2) - k_1][x_2(1 - q_0^2) - k_2] - [x_3(1 - q_0^2) - k_3]^2 \quad (2.23)$$

$$k_1 = y_1^2 - 2q_0y_1y_4 + y_4^2 \quad k_2 = y_2^2 - 2q_0y_2y_3 + y_3^2 \quad (2.24)$$

$$k_3 = y_1y_3 - q_0(y_1y_2 + y_3y_4) + y_2y_4$$

and we remind that $q_0 = q/\sqrt{q_1q_2}$. The saddle-point equations are easily solved numerically, while it is possible to check analytically that for $q_0 = 0$ we have $\Delta(E_1, E_2, 0) = \Xi(E_1) + \Xi(E_2)$ and then equation (2.6) is fulfilled.

3. Normal and anomalous regimes

In this section we analyse the dependence of the constrained complexity Σ_c on E_2 and q , at a fixed value of E_1 . In particular, we focus our attention on the dependence of Σ_c on the overlap q , since we are interested in the overlap spectrum of the system, which gives information on the geometrical distribution of the states in the phase space. In what follows it is always assumed $T \in [T_s, T_d]$, where T_s and T_d are respectively the static and the dynamical transition temperatures.

As a value for the reference energy E_1 we choose $E_1 = E_{\text{eq}}(\beta)$, where $E_{\text{eq}}(\beta)$ is the zero temperature energy density of those TAP solutions that dominate at temperature β ; in this way, we are fixing an equilibrium state and counting how many states of energy density E_2 are present at distance q from it. We stress, however, that we could choose any other value for the reference energy E_1 , obtaining qualitatively the same results.

It is useful to distinguish two different regimes: a *normal* regime, corresponding to values of E_2 well below the threshold, in which geometrical considerations at least

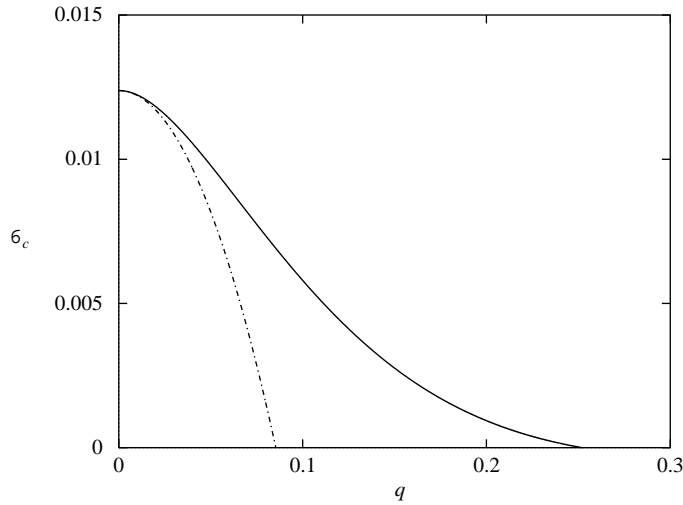


Figure 1. The constrained complexity Σ_c as a function of the overlap q (full curve), with $E_1 = E_2 = E_{\text{eq}} = -1.156$, for $\beta = 1.64$ and $p = 3$. The self overlap of the two states is $q_1 = q_2 = 0.55$, while $\Sigma_c = 0$ at $q_{\text{last}} = 0.25$. The chain curve is the curve predicted by a random distribution of the states (see the text). For $q = 0$ both the curves coincide with the unconstrained complexity $\Sigma(E_2)$.

qualitatively apply, and an *anomalous* regime, characterized by values of E_2 just below the threshold, which shows a rather peculiar behaviour of Σ_c .

3.1. The normal regime

The normal regime is defined by values of the energy E_2 of the states we are counting well below the threshold energy E_{th} . Intuitively, we expect that Σ_c decreases with increasing q , since larger values of q correspond to smaller portions of the phase space. This is indeed what happens in the normal regime, as shown in figure 1, where we have plotted Σ_c as a function of q .

The full curve of figure 1 provides us with some important information. First it is a *continuous* curve, meaning that there is a continuous spectrum of states with energy E_2 around the fixed reference state of energy E_1 (in the figure we have set $E_2 = E_{\text{eq}}$). This means that there is an exponentially high number of states at any value of q , until a value q_{last} for which $\Sigma_c = 0$. Thus q_{last} gives the overlap of the nearest states with energy E_2 . It is important that, as long as E_1 and E_2 are different from E_{th} , this value q_{last} is *smaller* than the self overlap of the considered states. This gap between the last value of the overlap in the spectrum and the self overlaps q_1, q_2 simply means that these states are well separated one with respect to the other, i.e.

$$\frac{q_{\text{last}}}{\sqrt{q_1 q_2}} < 1. \quad (3.1)$$

This has to be compared with the case of the SK model [1] in which, as well as in this case, there is a continuous distribution of states, but with a mutual overlap going from $q = 0$ up to the self overlap $q = q_{\text{EA}}$ [22, 23].

The second important feature of figure 1 can be caught if we compare Σ_c with the corresponding quantity that would be obtained in the case of a *random* distribution of the

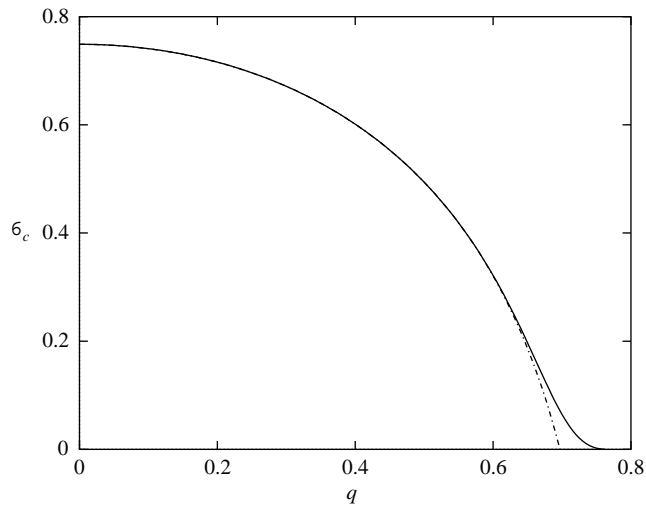


Figure 2. The constrained complexity Σ_c (full curve), compared with the random distribution (3.2) (chain curve) for $p = 30$. All other parameters are the same as in figure 1.

states. The simplest hypothesis we can formulate on the geometrical structure of the states is that they are randomly distributed in the phase space: in this case, the number of states at distance q from a given fixed point in the phase space would be simply given by the total number of states multiplied by the volume of the manifold defined by fixing q , i.e.

$$\Sigma_{\text{random}} = \Sigma(E_2) + \frac{1}{2} \log \left(1 - \frac{q^2}{q_1 q_2} \right) \quad (3.2)$$

where $\Sigma(E_2)$ is the unconstrained complexity and q_1, q_2 are the self overlaps of the two solutions. If we plot this quantity as a function of q and compare it with $\Sigma_c(q)$ (figure 1), it can be seen that there is a violation of the random distribution and that this violation goes in the direction of having a higher number of states when looking at small distances.

The comparison with the random distribution of the states suggests an interesting check. It is known that the p -spin model in the limit $p \rightarrow \infty$ coincides with the random energy model of [21], which is characterized by a complete decorrelation of the energy levels of the system. Therefore, we expect that for increasing values of p the constrained complexity Σ_c becomes increasingly similar to the random distribution (3.2). This is shown in figure 2, where we see that for $p = 30$ only a short tail remains for large q in which the two distributions are different, whereas, for $p \rightarrow \infty$ they coincide. We note that in the random energy model there is no geometrical structure at all. What we have here is that a complete *energetic* decorrelation between different states corresponds to a complete *geometrical* decorrelation in the phase space.

Finally we consider the dependence of Σ_c on the energy E_2 of the states that we are counting. In figure 3 we have plotted $\Sigma_c(E_2)$ at various values of q . The curve on the top corresponds to $q = 0$ and then reproduces the unconstrained complexity $\Sigma(E_2)$ (see equation (2.6)). We note that, even at fixed $q \neq 0$, Σ_c increases with increasing E_2 , as in the unconstrained case. Furthermore, as expected, the whole curve $\Sigma_c(E_2, q)$ decreases with increasing q .

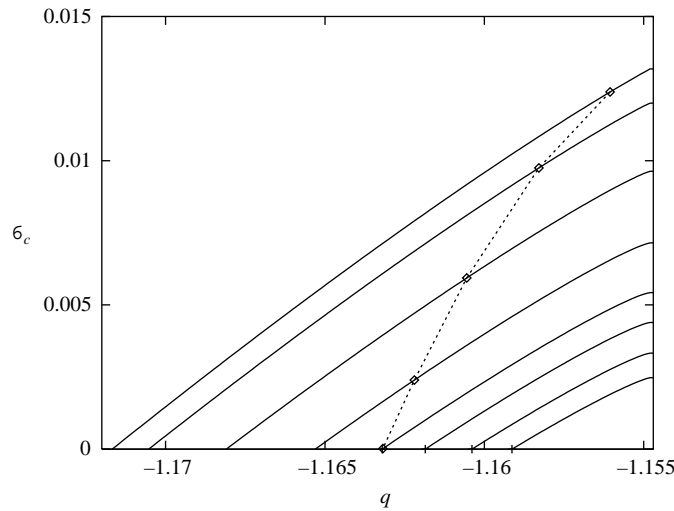


Figure 3. The constrained complexity Σ_c as a function of the energy E_2 , at various values of the overlap q and $E_1 = E_{eq} = -1.156$, for $\beta = 1.64$ and $p = 3$. The first curve on the top has $q = 0$ and thus corresponds to the unconstrained complexity $\Sigma(E_2)$. The threshold energy is $E_{th} = -1.1547$. The squares indicate the minimum of the function ϕ_c (see section 4), which reaches the axis $\Sigma_c = 0$ at $q_{low} = 0.113$.

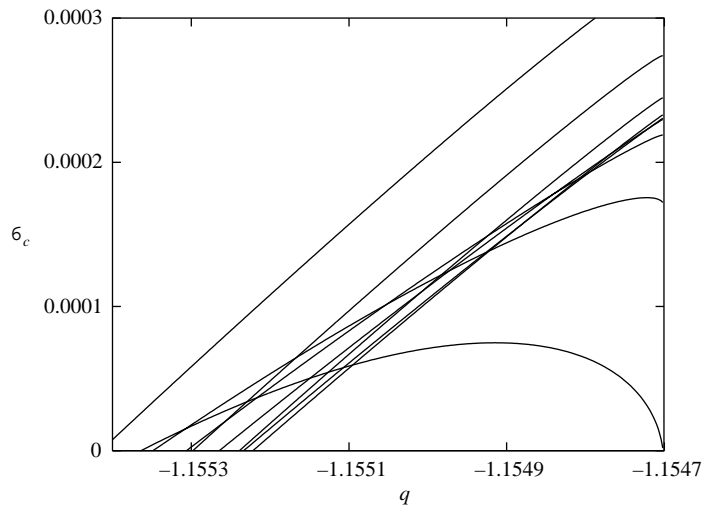


Figure 4. The constrained complexity Σ_c as a function of the energy E_2 just below the threshold, at various values of q . The value q_{max} corresponds to the curve whose intersection with the axis $\Sigma_c = 0$ starts going to the left with increasing q .

3.2. The anomalous regime

We turn now to the examination of the anomalous regime. If we plot Σ_c as a function of E_2 exactly as in figure 3, but now expanding a narrow range of energies E_2 just below the threshold ($E \in [E_{th} - 5 \times 10^{-4}, E_{th}]$), we obtain the behaviour shown in figure 4.

The curves get lower and lower with increasing q , until for a value of q that we call

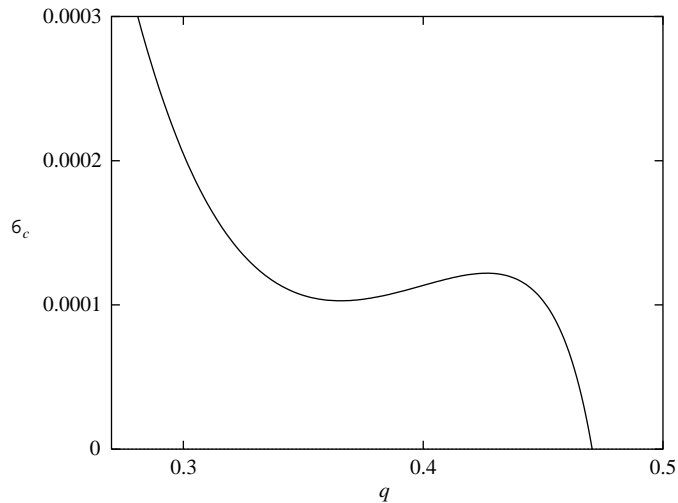


Figure 5. The constrained complexity Σ_c as a function of the overlap q in the anomalous regime. $E_1 = E_{\text{eq}}$ and $E_2 = -1.1550$.

q_{max} they begin to reverse, folding upwards. In figure 4, q_{max} corresponds to the curve whose intersection with the $\Sigma_c = 0$ axis starts going backward to the left with increasing q . If now we take a section of these curves at a fixed value of E_2 in this range, plotting Σ_c as a function of q , we find the anomalous behaviour of figure 5: there is an interval of q where Σ_c increases with increasing q .

The reversed behaviour of Σ_c clearly has no geometrical origin and for this reason we talk of an anomalous regime. What it seems is that, given a state (in this case an equilibrium state), there is a sort of clustering of states with high energy at small distances (large overlap) from it, thus giving the distribution of figure 5. Moreover, from figure 4 we note that for high enough values of q , Σ_c is no longer monotonic with respect to E_2 , and it develops a maximum. Therefore, in this range of q , threshold solutions are no longer the most numerous around the fixed equilibrium state.

To conclude, we note that the amplitude of the anomalous regime depends on the reference energy E_1 : the range of energies E_2 into which this anomalous behaviour occurs is larger for low values of E_1 and shrinks to zero as E_1 approaches E_{th} .

4. The spectrum of the dominant states

At a first sight the increasing of Σ_c with q , together with the role of q_{max} in the anomalous regime could seem an artefact of the calculation. Nevertheless, we are going to show that this behaviour is able to explain the energy spectra obtained with the real replica method of [15], where a completely different kind of computation is performed.

To face this problem we have to ask: Which are the *dominant* states at overlap q from a given fixed state? In the unconstrained case [8,9,11], equilibrium states of the system are defined as those TAP solutions that minimize the generalized free-energy density $\phi(f) = f - T\Sigma(f)$. Similarly, we can wonder which solutions dominate at distance q from a given equilibrium state. To this end we look for the minimum of the function $\phi_c(f, q) = f - T\Sigma_c(f, q)$, with $E_1 = E_{\text{eq}}$ and Σ_c expressed as a function of the free-energy density f of the states found at distance q . In figure 3, for each given value of

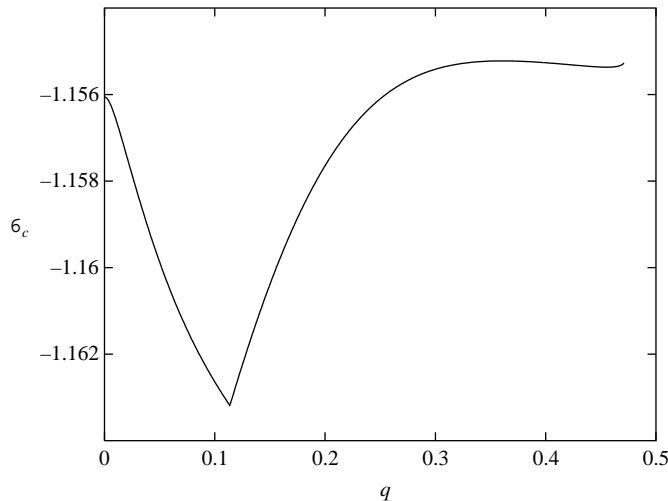


Figure 6. The energy density E_2 of the solutions dominating at distance q from the fixed equilibrium solution. The cuspid is at $q_{\text{low}} = 0.113$ and the maximum is at $q_{\text{max}} = 0.360$. The last point of the curve represents the distance of the nearest solutions.

q , we have signed on the corresponding curve the point that minimizes ϕ_c . As it is easily seen, there is a value of q for which the minimum of ϕ_c reaches the axis $\Sigma_c = 0$. We call this value q_{low} . If we look for a minimum of ϕ_c when $q > q_{\text{low}}$ we would be brought to a negative value of Σ_c , i.e. to non-existing solutions (in the limit $N \rightarrow \infty$). In this situation, the dominant solutions are those with the lowest energy density and a non-negative value of the complexity, i.e. with $\Sigma_c = 0$. Due to this, at q_{low} there is a sharp change in the energy behaviour of the dominant solutions: this energy decreases following the minimum of ϕ_c until $q = q_{\text{low}}$, then, for higher values of q , it increases following the intersection of the curves $\Sigma_c(E_2)$ with the axis $\Sigma_c = 0$. Yet, from figure 4 we see that when q reaches q_{max} , due to the anomalous behaviour of Σ_c this intersection point inverts its direction, and so the energy of the dominant solutions starts to decrease.

We conclude that the energy density of the solutions dominating at distance q from a fixed equilibrium state has a cuspid for $q = q_{\text{low}}$ and reaches a maximum at $q = q_{\text{max}}$. The above is all shown by figure 6.

In the real replica method usually a first replica is quenched into an equilibrium state, while a second replica is forced to thermalize at distance q from it [10, 15]. It is then natural to think that the second replica thermalizes into one of the states that dominate at distance q in the sense described above, and that therefore the spectrum of the states visited by this second replica is of the same kind as the spectrum of figure 6. This is indeed what happens, as shown in more detail in the appendix: the spectrum found with the real replica method of [15] presents a cuspid, and has a maximum exactly at $q = q_{\text{max}}$, thus providing confirmation of the existence of the anomalous regime.

In analysing figure 6 it is important to note that the number of dominant states is exponentially high in N as long as $q < q_{\text{low}}$, while it is of order N for $q > q_{\text{low}}$. In terms of constrained systems this transition is signalled by the breaking of the replica symmetry in the overlap matrix giving further confirmation of the consistency of these two different methods (see the appendix) [15, 20].

The ending point of this curve corresponds to that value of the overlap above which no

states of any energy are found with $\Sigma_c \geq 0$. Thus it indicates which is the overlap with the fixed state of energy $E_1 = E_{\text{eq}}$ of the states nearest to it. It turns out that these nearest states have an energy density *greater* than the energy E_{eq} of the fixed reference state, even if in general they are not threshold states. What is important is that this is not a special feature of the equilibrium states: indeed, given a state of *any* energy E_1 , the states nearest to it *always* have an energy density greater than E_1 .

This behaviour is not a trivial consequence of the fact that states with higher energy are in general more numerous, since following this reasoning the nearest states would always be the threshold ones (which have the greatest unconstrained complexity), while we know that this is not true. Indeed, as mentioned in section 3, at large values of the overlap q , i.e. in the anomalous regime, threshold states are no longer the most numerous around a given fixed state. Once the curve of the dominant states of figure 6 develops a maximum at q_{max} , it is not obvious which should be the energy of the states corresponding to the ending point of this curve.

5. The threshold states

We turn now to examine the structure of the threshold states. We recall that threshold states are those solutions of the TAP equations with the highest energy density E_{th} . These states have a great importance under several aspects.

From a static point of view it can be shown that threshold states are *marginal*: the typical spectrum of the free-energy Hessian evaluated in a TAP solution of energy E is a semicircle with support in the positive semi-axis and its lowest eigenvalue λ_{min} goes to zero as E goes to E_{th} . In this sense threshold states develop some flat directions.

On the other hand, in the temperature range $T < T_d$, threshold states play a fundamental role in the off-equilibrium dynamics of this model. Solving analytically the dynamical equations with random initial conditions (i.e. high-energy initial conditions), one finds that the asymptotic limit of the energy \mathcal{E}_{∞} coincides with the threshold energy E_{th} . In other words, the asymptotic dynamics takes place at the threshold level, never visiting the subthreshold landscape. Moreover, the dynamical evolution of the system presents a first equilibrium regime in which the correlation function goes to the value of the self overlap of the threshold states q_{th} , followed by an off-equilibrium aging regime in which the correlation function goes to zero. This means that the system never truly thermalizes into any of the threshold states, but that rather it continuously drifts away [6].

Therefore, it is intriguing to investigate the eventual relations between the peculiar dynamical behaviour that occurs at the threshold level and the geometrical structure of the threshold states.

To perform an analysis of this kind we set $E_1 = E_2 = E_{\text{th}}$, and we study the constrained complexity Σ_c as a function of q , i.e. we fix a threshold solution and count how many other threshold solutions are present at a distance q from it. The corresponding curve is shown in figure 7.

The important result is that

$$\Sigma_c(q) \rightarrow 0 \quad \text{for } q \rightarrow q_{\text{th}}(\beta) \quad (5.1)$$

where $q_{\text{th}}(\beta)$ is the self overlap of the threshold states at the temperature β we are considering. More precisely we find

$$\Sigma_c(q) \sim (q_{\text{th}} - q)^5 \quad \text{for } q \sim q_{\text{th}}. \quad (5.2)$$

When the overlap between two states of the same kind is equal to their self overlap, it means that these two states are coincident in the thermodynamic limit. Thus, thinking

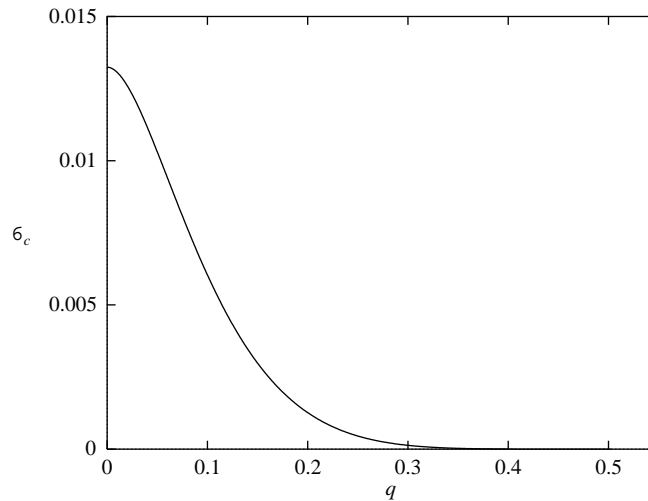


Figure 7. The constrained complexity Σ_c as a function of q with $E_1 = E_2 = E_{\text{th}}$, for $\beta = 1.64$ and $p = 3$. For $q > 0.35$ the curve is indistinguishable from the axis and it reaches zero for $q = q_{\text{th}} = 0.504$.

of well separated states, one expects that Σ_c goes to zero at a value of q which is lower than the self overlap: indeed this is what happens for all the states below the threshold (see figure 1 and equation (3.1)).

On the other hand, from (5.1) we see that when fixing a threshold state, other threshold states with vanishing complexity are found until a distance zero from the fixed one. A similar conclusion was deduced in [15], but in that context it was possible to state this result only at the dynamical transition temperature $\beta = \beta_d$, at which threshold states are the equilibrium ones. Here we see that this remains true at any temperature, as a natural consequence of the non-chaoticity of TAP solutions with temperature.

As a consequence of equation (5.1) we can say that there is no sharp separation among threshold states, and that they rather form a structure of coalescent states. This means that these states are separated by free-energy *density* barriers which are vanishing in the limit $N \rightarrow \infty$, i.e. that the free-energy barriers grow as N^α with $\alpha < 1$ [26].

As previously said, these states are minima of the TAP free energy with some flat directions. We can then argue that they are connected along these flat directions, forming a sort of channel of states. Into this frame the dynamical drifting of the system (i.e. the decreasing to zero of the correlation function in the off-equilibrium regime) can be viewed as a wandering along this channel of threshold states, in agreement with the ideas outlined in [6].

Finally, we note that, due to equation (5.1), the distribution of threshold states has no gap between the last value of the overlap in the spectrum and the self overlap, unlike all other subthreshold states. This feature is reminiscent of the overlap distribution in the SK model. Besides, we recall that in the SK model all the states are marginal, as happens for the threshold states in the p -spin spherical model. From this point of view, we can say that threshold states are the most SK like.

6. Conclusions and open questions

The p -spin spherical model for $T_s < T < T_d$ is dominated by an exponentially high number of states, each one having a rather high free-energy density f and therefore very small weight. This high free-energy is counterbalanced by the entropic contribution of the complexity. Besides these equilibrium states, there is a great variety of metastable states, with free-energy densities both lower and larger than the equilibrium one, all having a vanishing weight. In this sense, there is no real difference between equilibrium and metastable states, being the equilibrium condition of a collective property.

In this situation, the standard replica approach fails, since it is not able to discriminate the overlap relations among all these states, while the TAP approach gives no information on the overlap distribution of them.

We have faced this problem introducing an overlap q between different TAP solutions and performing a purely entropic computation of their number. In this way we have defined a constrained complexity $\Sigma_c(q)$, which plays the role of the overlap distribution of the states.

By means of Σ_c we have found that the states are disposed in a non-trivial way: fixed an arbitrary state from where observing the phase space, there is a continuous spectrum of states surrounding it. This means that there are states at each value of the overlap q with the reference one, from $q = 0$ until a maximum value q_{last} . For subthreshold states there is a gap between this last value of the overlap and the value of the self overlap, meaning that they are well separated states. Moreover, the distribution is different from the one obtained supposing a random distribution of the states, since it shows a major crowding of states at small distances. Yet, the two distributions coincide in the $p \rightarrow \infty$ limit, when the case of the random energy model is recovered.

Furthermore, the analysis of threshold states has given some interesting results: these marginal states have an overlap distribution which goes continuously to zero at a value of q equal to their self overlap q_{th} . This means that these states are connected along their flat directions, forming a sort of channel that winds along the phase space. This feature may have a role in the asymptotic dynamics of the system, which occurs at the level of the threshold landscape.

To comment on the continuous distribution of the overlap, and in particular the coalescent structure of the threshold states, we have often referred to the SK model, for which a continuous structure with respect to the overlap q is directly given by the standard distribution function $P(q)$. However, in doing this comparison it is necessary to make some specifications. In the ultrametric structure of the SK model the main role is played by the equilibrium states, which have the lowest free energy and finite weight, and whose number is of order N . This means that one can disregard the exponentially high number of states with higher free energy and vanishing weight (this can be done by introducing a cut-off on the branches size of the ultrametric tree [24]). The situation for the p -spin spherical model is somehow the opposite: here the states, both of equilibrium and metastable, *all* have vanishing weight and are in exponentially high number. Therefore none of these states, whatever energy it has, can be disregarded. In this sense the investigation of the structure of the states for this model is complicated by the existence of a new relevant variable, that is the energy.

Moreover, we stress that, at the present moment, there is no evidence of an ultrametric organization of the states in the p -spin spherical model. To investigate this point it would be necessary to analyse the correlation among triplets of states, as it has been done for the SK model in [22]. The only fair indication of a clustering structure of the states comes

from the existence of the anomalous regime, into which the constrained complexity grows with the overlap q . The existence of this anomalous regime is confirmed by the real replica method.

By means of the constrained complexity we have also obtained the spectrum of the dominant states at distance q from a given fixed state. This spectrum shows that below a certain value of the overlap, the number of the dominating states is exponential in N , while above this value (close states) this number is of order N . Besides, we have seen that the states nearest to any given state always have higher energy density.

We want to mention here a working hypothesis that could be useful for the present investigation. In the generalized random energy model of [25], an ultrametric structure is directly built in by defining the probability distributions of the energies at each clustering level. In this context, an equivalent of the functional order parameter $x(q)$ of [3, 4] can be identified. In [25] this construction is explicitly performed in the case of two clustering levels: in this simple example one can see that a function $x(q)$ which *decreases* with increasing q corresponds to a hidden ultrametric structure, in the sense that this structure is present by construction, but is not revealed from the computation of the free energy of the system. This suggests that for the p -spin spherical model also, where a rich distribution of states is present but hard to reveal, an anomalous function $x(q)$ could describe the underlying hidden structure. The existence of anomalous solutions of this kind in the context of the replica approach has been shown and discussed in [9, 13, 27, 28].

To conclude, the main open issue on this topic is the pursuit of a unifying frame where it is possible to insert all the obtained results in order to describe, in a synthetic way, the rich and complex structure of states of the p -spin spherical model.

Acknowledgments

It is a pleasure to thank Alain Barrat, Leticia Cugliandolo, Silvio Franz, Jorge Kurchan, Marc Mézard, Rémi Monasson, Heiko Rieger, Felix Ritort and Miguel Angel Virasoro for their important suggestions and very useful discussions.

Appendix: The comparison with the real replica method

The real replica method [9, 10, 15, 17] consists of studying the static properties of a certain number of real replicas of the system, as a function of the overlaps imposed among them. In [15] we introduced a three-replica potential by which we analysed the structure of equilibrium and metastable states of the p -spin spherical model: the first replica is fixed into an equilibrium state, while the second replica is forced to equilibrate at overlap q_{12} with the first one. Clearly, the way in which replica 2 chooses its constrained equilibrium state is heavily conditioned by the complexity Σ_c of the states at that distance. Having fixed replicas 1 and 2, the potential V_3 is defined as the free-energy density of a third replica as a function of its distances q_{13} and q_{23} from the first two. The most important minimum of V_3 corresponds to replica 3 in local equilibrium into the state chosen by replica 2. In this minimum, which we call M_2 , the energy and the self overlap of replica 3 satisfy TAP equations, meaning that replicas 2 and 3 have found a state of the unconstrained system at distance q_{12} from the equilibrium state of replica 1.

Before proceeding further it is crucial to clarify the different roles of the three replicas, beginning from the way in which replica 2 chooses the state at distance q_{12} from 1. If the TAP free energy is minimized *on* the manifold defined by fixing q_{12} , the number of

minima found is clearly greater than the number of *genuine* TAP solutions at that distance and for the most part consists of projections on the manifold of nearby true TAP solutions. These projections are what replica 2 sees as states. Therefore, we can say that replica 2 thermalizes in the vicinity of a TAP solution, but this solution is in general at distance $q \neq q_{12}$ from replica 1. On the other hand, this TAP solution is that into which replica 3 thermalizes giving the minimum M_2 , and this is why replica 3 gives the right TAP energy of this state and its right distance from replica 1, while replica 2 does not. To understand the energy spectrum of the states visited by replica 3, we must then investigate how replica 2 chooses these states.

As usual, replica 2 tries to optimize the balance between the free energy and the complexity of the solutions it finds on the manifold, minimizing a function $\phi_2 = f_2 - T\Sigma_2(f_2, q_{12})$. It is important to note that Σ_2 is *not* the same function as Σ_c . There are *many* genuine TAP solutions with different TAP free energies f and at slightly different distances q , either higher or lower than q_{12} , whose projections on the manifold of replica 2 all have the same free energy f_2 . Of these TAP solutions the relevant ones are those with the maximum complexity $\Sigma_c(f, q)$. This maximum value will then give $\Sigma_2(f_2, q_{12})$. Summarizing, $\Sigma_2(f_2, q_{12})$ is equal to the complexity Σ_c of the most numerous TAP solutions whose projections on the manifold fixed by q_{12} have free energy f_2 (the computation of Σ_2 is explicitly performed in [20]).

The minimization of ϕ_2 with respect to f_2 then selects a particular class of TAP solutions. Using the distorted method explained above, replica 2 is quenched into one of these solutions, while replica 3 truly thermalizes into it. For this reason, the dependence on q_{12} of the energy of replica 3 in the minimum M_2 is a mere manifestation of the process of equilibration of replica 2 above.

Resuming, the states visited by replica 3 are chosen minimizing ϕ_2 , which does not coincide with the function ϕ_c of section 4; also Σ_2 is not the same function as Σ_c . Nevertheless, it is clear that the spectrum given by the minimization of ϕ_2 must be similar to the one given by ϕ_c in section 4.

To make then a comparison with figure 6, it is convenient to plot the zero-temperature energy of replica 3 in the minimum M_2 as a function of the overlap q_{13} , instead of q_{12} , since, as stated above, q_{13} better represents the real overlap between the two states. This parametrization is possible because in the minimum M_2 the values of q_{13} is uniquely determined by q_{12} .

It can be seen from a comparison between figures 6 and A.1 that, as we expected, the processes of minimization of ϕ_c and ϕ_2 are qualitatively the same. First, we note from figure A.1 that there is a value of q_{13} for which the curve has a cuspid; we call the corresponding value of q_{12} in the minimum M_2 for which this cuspid occurs, q_{rsb} . Indeed, following the same line of reasoning of section 4, we argue that this cuspid must correspond with the point in which Σ_2 becomes zero. The computation developed in [15,20] shows that for a value of q_{12} greater than q_{rsb} the overlap matrix \mathbf{Q}^{22} of replica 2 breaks the replica symmetry. Physically, an RS form of the overlap matrix means either that the systems find an exponentially high number of states (as in the p -spin model for $T_s < T < T_d$), or that the phase space consists in just one state (as in the paramagnetic case). On the other hand, an RSB form means that the phase space is dominated by a number of order N of states (as in the p -spin model for $T < T_s$). Therefore, the breaking of the replica symmetry of \mathbf{Q}^{22} for $q_{12} = q_{\text{rsb}}$ is a strong indication that replica 2 ceases to see an exponentially high number of dominant states here and confirms that, at this point, Σ_2 becomes zero, as we argued above. As already stressed, the functions ϕ_2 and ϕ_c , even though they have a similar physical meaning, are actually different and this is why the corresponding minimization curves (first

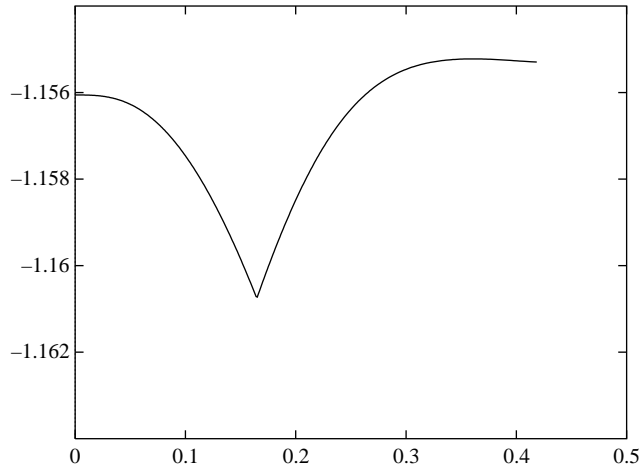


Figure A.1. The energy density E of replica 3 in the minimum M_2 of the three-replica potential, as a function of the overlap q_{13} , for $\beta = 1.64$ and $p = 3$. Here, as in figure 6, $q_{\max} = 0.360$.

branches in figures 6 and A.1) are different.

Secondly, in figure A.1 we note a maximum for $q_{13} = q_{\max}$, i.e. exactly at the same point as in figure 6. This is a consequence of the reversing in the behaviour of Σ_c that occurs in the anomalous regime. This behaviour is directly inherited by Σ_2 : loosely speaking, if there are TAP solutions whose number starts to increase getting closer to the state of replica 1, the corresponding projections on a fixed manifold will also increase. This is an important confirmation of the role of the quantity q_{\max} and, as a consequence, it is a confirmation of the existence of the anomalous regime.

Finally, it is worth observing that the ending points of the two curves are different, i.e. the potential V_3 ceases to see states around replica 1 at a distance that is *greater* than the one corresponding to the nearest TAP solutions given by Σ_c . This can signify either that the potential fails to see these last states because replica 2 does not thermalize in the vicinity of them, or that these last solutions given by Σ_c actually are not minima of the TAP free energy. At the present moment this is an open question.

Summarizing the considerations of this appendix we can say that the energy spectrum given by the real replica method is well explained by the behaviour of the constrained complexity. This mutually confirms the results found with the two methods.

References

- [1] Sherrington D and Kirkpatrick S 1975 *Phys. Rev. Lett.* **35** 1792
- [2] Thouless D J, Anderson P W and Palmer R G 1977 *Philos. Mag.* **35** 593
- [3] Parisi G 1979 *Phys. Rev. Lett.* **23** 1754
- [4] Parisi G 1980 *J. Phys. A: Math. Gen.* **13** L115
- [5] Parisi G 1980 *J. Phys. A: Math. Gen.* **13** 1887
- [6] Cugliandolo L F and Kurchan J 1993 *Phys. Rev. Lett.* **71** 173
- [7] Kirkpatrick T R and Thirumalai D 1987 *Phys. Rev. B* **36** 5388
- [8] Crisanti A and Sommers H-J 1992 *Z. Phys. B* **87** 341
- [9] Kurchan J, Parisi G and Virasoro M A 1993 *J. Phys. I* **3** 1819
- [10] Franz S and Parisi G 1995 *J. Phys. I* **5** 1401
- [11] Barrat A, Burioni R and Mézard M 1996 *J. Phys. A: Math. Gen.* **29** L81
- [12] Crisanti A and Sommers H-J 1995 *J. Phys. I* **5** 805

- [13] Virasoro M A 1996 Simulated annealing methods under analytical control *Statphys 19 Proc. 19th IUPAP Int. Conf. Stat. Phys., Xiamen, China* ed B-L Hao (Singapore: World Scientific)
- [14] Gross D J and Mézard M 1984 *Nucl. Phys. B* **240** 431
- [15] Cavagna A, Giardina I and Parisi G 1996 *J. Phys. A: Math. Gen.* **30** 4449
- [16] Bray A J and Moore M A 1980 *J. Phys. C: Solid State Phys.* **13** L469
- [17] Franz S, Parisi G and Virasoro M A 1992 *J. Phys. I* **2** 1869
- [18] Kurchan J 1991 *J. Phys. A: Math. Gen.* **24** 4969
- [19] Vertechi D and Virasoro M A 1989 *J. Physique* **50** 2325
- [20] Barrat A, Franz S and Parisi G 1997 *J. Phys. A: Math. Gen.* **30** 5593
- [21] Derrida B 1981 *Phys. Rev.* **B 24** 2613
- [22] Mézard M, Parisi G, Sourlas N, Toulouse G and Virasoro M A 1984 *J. Physique* **45** 843
- [23] Mézard M, Parisi G and Virasoro M A 1987 *Spin Glass Theory And Beyond* (Singapore: World Scientific)
- [24] Ruelle D 1987 *Commun. Math. Phys.* **108** 225
- [25] Derrida B 1985 *J. Physique* **46** L401
- [26] Kurchan J and Laloux L 1996 *J. Phys. A: Math. Gen.* **29** 1929
- [27] Baviera R 1995 Tesi di Laurea, Università degli Studi di Roma 'La Sapienza'
- [28] Ferrero M E 1993 Tesi di Laurea, Università degli Studi di Roma 'La Sapienza'